





Gamma-Ray Burst in a Binary System

ZE-CHENG ZOU (邹泽城) ¹, BIN-BIN ZHANG ^{1,2,3}, YONG-FENG HUANG (黄永锋) ^{1,2} AND
XIAO-HONG ZHAO (赵晓红) ^{4,5}

¹*School of Astronomy and Space Science, Nanjing University, Nanjing 210023, China*

²*Key Laboratory of Modern Astronomy and Astrophysics (Nanjing University), Ministry of Education, Nanjing 210023, China*

³*Department of Physics and Astronomy, University of Nevada Las Vegas, NV 89154, USA*

⁴*Yunnan Observatories, Chinese Academy of Sciences, 650216, Kunming, China*

⁵*Center for Astronomical Mega-Science, Chinese Academy of Sciences, Beijing, China*

(Dated: August 5, 2021)

Submitted to ApJ

ABSTRACT

Regardless of their different types of progenitors and central engines, gamma-ray bursts (GRBs) were always assumed to be standalone systems after they formed. Little attention has been paid to the possibility that a stellar companion can still accompany a GRB itself. This paper investigates such a GRB-involved binary system and studies the effects of the stellar companion on the observed GRB emission when it is located inside the jet opening angle. Assuming a typical emission radius of $\sim 10^{15}$ cm, we show that the blockage by a companion star with a radius of $R_c \sim 67 R_\odot$ becomes non-negligible when it is located within a typical GRB jet opening angle (e.g., ~ 10 degrees) and beyond the GRB emission site. In such a case, an on-axis observer will see a GRB with a similar temporal behavior but 25% dimmer. On the other hand, an off-axis observer outside the jet opening angle (hence missed the original GRB) can see a delayed “reflected” GRB, which is much fainter in brightness, much wider in the temporal profile and slightly softer in energy. Our study can naturally explain the origin of some low-luminosity GRBs. Moreover, we also point out that the companion star may be shocked if it is located inside the GRB emission site, which can give rise to an X-ray transient or a GRB followed by a delayed X-ray bump on top of X-ray afterglows.

Keywords: Binary stars (154) — Gamma-ray bursts (629)

1. INTRODUCTION

Gamma-ray bursts (GRBs) represent the most high-energy transients in the universe, with the isotropic bolometric emission energy, E_{iso} , ranging from $\sim 10^{46}$ erg to $\sim 10^{55}$ erg (Zhang 2018). The prompt emis-

sion of a GRB is believed to be generated by a relativistic jet launched from the central engine, while the afterglow is likely produced by external shocks from the interaction between the jet material and circumburst medium (for a review, see Kumar & Zhang 2015).

GRBs are traditionally classified into long or short events according to their durations (Kouveliotou et al. 1993). The progenitors of short GRBs have long been believed to be mergers involving neutron stars (e.g., Eichler et al. 1989; Narayan et al. 1992; Nakar 2007) and are finally confirmed through GW170817/GRB 170817A association (Abbott et al. 2017a,b). It is interesting to note that neutron stars may actually be strange quark stars (Geng et al. 2021). On the other hand, long GRBs

Corresponding author: Ze-Cheng Zou
zou.ze-cheng@smail.nju.edu.cn

Corresponding author: Bin-Bin Zhang
bbzhang@nju.edu.cn

Corresponding author: Yong-Feng Huang
hyf@nju.edu.cn

are identified as dying massive stars (van Paradijs et al. 1997; Costa et al. 1997; Frail et al. 1997), among which the most popular candidates are Wolf-Rayet (WR) stars (Woosley 1993). In the so-called “collapsar” model, the core of a dying WR star is required to rotate very fast to launch a relativistic jet (MacFadyen & Woosley 1999), though how to spin it up has been long debated (for a review, see Levan et al. 2016).

Many stars are in binary or even multiple systems (Duchêne & Kraus 2013; Badenes et al. 2018). Therefore, one may naturally expect that the progenitors of GRBs can be part of such systems. Binary star progenitors of long GRBs have been previously investigated by many authors (e.g., Izzard et al. 2004; Fryer & Heger 2005; Petrovic et al. 2005; Woosley & Heger 2006; Cantiello et al. 2007; de Mink et al. 2009). The binary interaction can significantly change the characteristics of the GRB progenitor. In this so-called binary star scenario, a massive star is spun up by its close companion via mass transfer and/or tidal forces to produce a GRB (Fryer & Heger 2005; Woosley & Heger 2006; Cantiello et al. 2007). It is interesting to note that a massive WR star in a binary system was recently reported (Callingham et al. 2019), which may potentially provide a long-duration GRB progenitor. On the other hand, the massive star can also be in a wide binary, where the system has a weak interaction. Hence, the progenitor is in fact an effectively single star, which can generate a GRB via chemically homogeneous evolution (e.g., Yoon & Langer 2005; Woosley & Heger 2006; Yoon et al. 2012).

On the other hand, a GRB is always assumed to be a standalone system after it is formed. The prompt emission of GRBs is usually thought to be of internal origin, so the central engine itself determines most of the observed properties. In this scenario, the existence of a stellar companion, if any, is ignored. Some early efforts (e.g., London & Cominsky 1983; Rappaport & Joss 1985; Dermer et al. 1991) have been made to predict that the reprocessing of the original GRB photons by nearby stars can produce an optical or X-ray counterpart with a time scale ranging from ~ 1 s to $\sim 10^3$ s. However, the case that a GRB is produced with a stellar companion located inside the jet opening angle has never been studied. In this paper, we will discuss such scenarios in detail. As shown below, the companion can occult or reflect the emission of the GRB, depending on the viewing angle of the observer. The GRB light curve and spectrum will therefore be modified.

This paper studies in detail the possible effects when a GRB happens in a binary system. Two types of effects, namely occultation and reflection, are proposed

and investigated. In Section 2, we describe the basic framework of the binary system. The observational effects of the stellar companion are presented in Section 3. Finally, we briefly conclude and discuss our results in Section 4. Throughout this paper, a flat Λ CDM cosmology with $H_0 = 67.4 \text{ km s}^{-1} \text{ Mpc}^{-1}$ and $\Omega_m = 0.315$ is adopted (Planck Collaboration et al. 2020).

2. BINARY CONFIGURATION

In this paper, the term “binary” refers to a system consisting of a primary object producing a GRB and its stellar companion, i.e., we do not specify a certain progenitor for the GRB. Nevertheless, since WR stars are the most popular candidate progenitors for long GRBs (Woosley 1993), we consult the Galactic Wolf Rayet Catalogue¹ (v1.25, Aug 2020; Rosslowe & Crowther 2015) to estimate the binarity fraction of WR stars in the Milky Way (MW). The catalog contains 667 Galactic WR stars, among which there are 103 WR stars in binary, yielding a fraction around 15%. Due to the usage of a different and updated database, our result is lower than those in the previous work (e.g., 39%; van der Hucht 2001), still being a significant number and indicating that a large amount of WR stars are in binary systems. Moreover, the binary fraction of WR stars in the Large Magellanic Cloud (LMC) is found to be 16% (or 36% with the unconfirmed candidates being taken into account; Hainich et al. 2014), and 40% in the Small Magellanic Cloud (SMC; Shenar et al. 2016). The above facts suggest that in the local universe, many WR stars can be found in binary systems for MW-like, LMC-like, and SMC-like metallicity. Assuming all WR stars collapse and lead to GRB events, we can reasonably conclude that the fraction that a GRB happens in a binary system, f_{bin} , is not a small number and can be as high as 50% (Mason et al. 2009; Lu et al. 2015). Considering that not all GRBs are collapsar GRBs, for simplicity, here we use an estimated $f_{\text{bin}} \sim 0.2$ to carry out our calculations in this paper.

A crucial parameter in the binary system is the separation (d) between the stellar companion and the GRB central engine. Some early studies (e.g., Paczyński 1967) suggested that WR stars can form through close binary evolution, while recent observations show that most Galactic WR binaries seem to have orbital periods longer than 100 days (Dsilva et al. 2020), corresponding to $d > 1.7 \times 10^{13}$ cm for 20 M_\odot circular binaries. An extreme example is the Apep system, which has an orbital period possibly longer than 10^4 years (Callingham et al. 2019). Indeed, Petrovic et al. (2005) claimed

¹ <http://pacrowther.staff.shef.ac.uk/WRcat/>

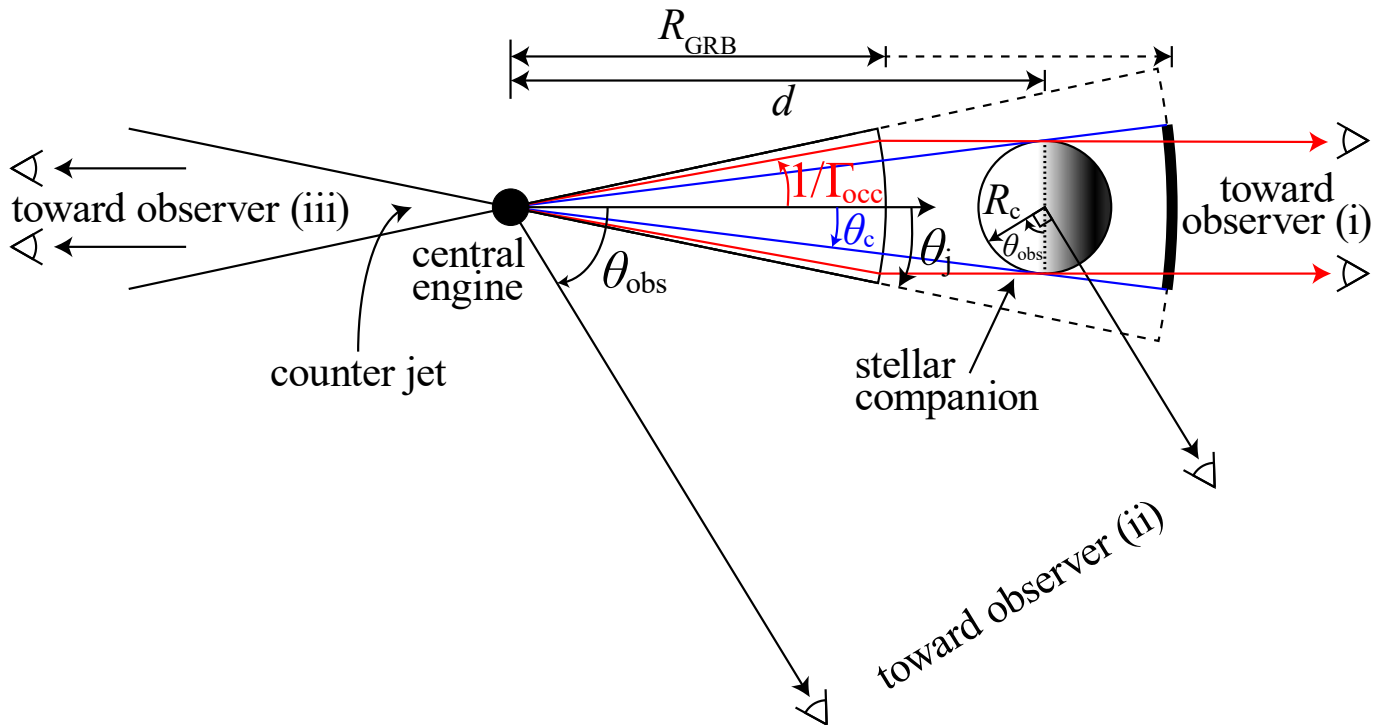


Figure 1. A not-to-scale sketch of the binary geometry with the stellar companion located inside the jet opening angle. Sectors with thin solid and dashed boundaries in black represent jets with emission sites within and beyond the companion, respectively. The thick solid black curve indicates the section occulted by the companion. Red and blue lines correspondingly indicate the definitions of Γ_{occ} and θ_c . For convenience, the companion is placed at the exact center of the jet. The dotted line divides the companion into a left irradiated hemisphere and a right nonirradiated hemisphere. For the observer, three cases are illustrated: (i) an on-axis observer, (ii) an observer with a viewing angle of θ_{obs} , and (iii) an observer located inside the counter jet.

that the interacting binary progenitor model is necessary to spin up the WR star core to produce a long GRB. Nevertheless, whether the binary is interacting or not is no longer critical when the magnetic torque is involved (Petrovic et al. 2005; Heger et al. 2005). Due to these uncertainties, we take d as a free parameter. We mainly study the case that d is larger than the GRB emission radius (R_{GRB}), but will also briefly discuss the case of $d < R_{\text{GRB}}$ (§3.4–3.6).

As illustrated in Figure 1, we assume that the stellar companion locates within the GRB jet opening angle, θ_j ; otherwise, the observational effect will be insignificant. This is theoretically possible (Horvat et al. 2018; Justesen & Albrecht 2020). In addition, we assume a random direction of the stellar companion when determining the observed event rates of such binary systems.

On the other hand, the observing angle (i.e., the angle between our line of sight and the jet direction) is a key parameter in our framework. As discussed below, an on-axis observer will see a dimmer GRB due to the occultation by the stellar companion (when $d < R_{\text{GRB}}$), whereas an off-axis observer will see a reflected and delayed GRB even though the original GRB is missed due to a large observing angle.

The framework we set up in this study involves a highly beamed central engine and a stellar companion. Besides a WR star, the progenitor of such a GRB central engine can, in principle, also be a compact star merger (e.g., two neutron stars or a neutron star and a black hole). In this case, we have a hierarchical trinary system before the merge phase, which is quite possible in dense star clusters (Fragione et al. 2020). Of course, some additional effects, such as a large kick velocity (up to $\sim 1000 \text{ km s}^{-1}$ for binary black hole mergers; e.g., Favata et al. 2004; Merritt et al. 2004; González et al. 2007; van Meter et al. 2010) caused by gravitational wave radiation (Fitchett 1983) may be unignorable, yet they are beyond the scope of this paper. In any case, the framework and theoretical calculations in this study can also apply to merger-origin short GRBs as long as the central engine and binary configuration are similar.

3. OCCULTATION AND REFLECTION EFFECTS

As discussed above, we only consider the situations when the stellar companion locates within the opening angle of the GRB jet. With the uncertainties of the distance between the GRB central engine and the companion as well as the observer's angle, we need to consider

Table 1. Six Different Cases of Binary Geometry

Case	d vs. R_{GRB}	Observer	Sections
I	$d \geq R_{\text{GRB}}$	on-axis	§3.1
II	$d \geq R_{\text{GRB}}$	off-axis	§3.2
III	$d \geq R_{\text{GRB}}$	counter-on-axis	§3.3
IV	$d < R_{\text{GRB}}$	on-axis	§3.4
V	$d < R_{\text{GRB}}$	off-axis	§3.5
VI	$d < R_{\text{GRB}}$	counter-on-axis	§3.6

six different cases of the system configuration (Table 1), which will be studied respectively in the following.

3.1. Case I

In this case, the GRB emission radius (R_{GRB}) is less than the separation between the GRB central engine and the companion, and the observer is on-axis (observer i in Figure 1). Depending on the blockage portion of the jet, the observer will see either a dimmer GRB or completely miss it.

For simplicity, we assume a uniform jet with a bulk Lorentz factor of Γ . Due to the relativistic beaming effect, only those photons emitted within a cone of $1/\Gamma$ can be observed. Thus the occultation calculation should be based on the comparison between $1/\Gamma$ and R_c/R_{GRB} , the latter defining the maximal possible blockage by the companion.

In order to calculate the condition for a total occultation, it is convenient to define a critical Lorentz factor of $\Gamma_{\text{occ}} \equiv R_{\text{GRB}}/R_c$. Considering the GRB framework, Γ_{occ} can be a few hundred. Taking $\Gamma_{\text{occ}} = 250$ as an example, we can further calculate its corresponding scales of the companion and the GRB radius to be $R_c = 67 R_{\odot}$ and $R_{\text{GRB}} = 10^{15}$ cm, with the latter being a typical GRB emission radius for a Poynting flux outflow (Zhang & Yan 2011) dominated ejecta. In fact, the initial Lorentz factor of some GRBs can indeed exceed 250 (e.g., Liang et al. 2010; Huang et al. 2020; Zhang et al. 2021). Therefore, our calculation suggests that the stellar companion can block the whole GRB prompt emission if Γ does not decrease much in the prompt emission phase. The prompt emission is unobservable, but the afterglow, with much smaller values of Γ , can still be observed as an orphan afterglow (e.g., Rhoads 1997; Huang et al. 2002).

On the other hand, the Lorentz factor of GRB ejecta can vary in a broad range (e.g., Liang et al. 2010) and is not necessarily identical to Γ_{occ} . So it is more likely that a partial occultation can occur when $\Gamma < \Gamma_{\text{occ}}$. In this

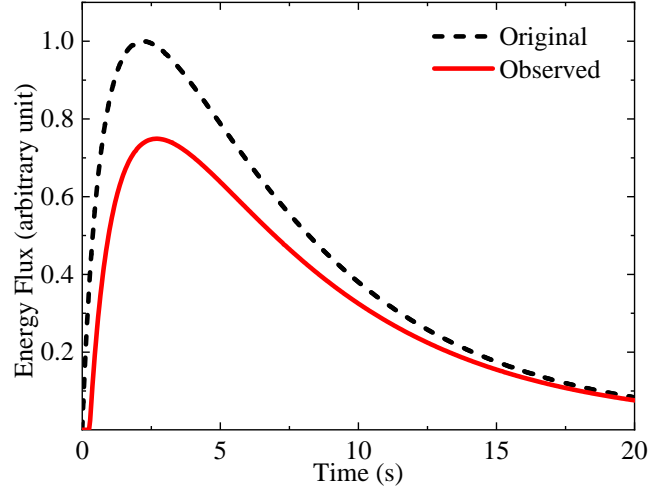


Figure 2. Original (dashed curve) and observed post-occultation (solid curve) light curves of a typical GRB. The light curves are normalized so that the peak flux of the original light curve equals to unity.

case, the GRB prompt emission still can be observed but at a much-reduced level. To study such occulted GRB light curves, we must include the curvature effect of the relativistic spherical shell (e.g., Ryde & Petrosian 2002; Kocevski et al. 2003; Dermer 2004; Uhm & Zhang 2015). For simplicity, we ignore the details of the radiation mechanisms (Geng et al. 2018b) but only consider the pure geometric effect. Following Ryde & Petrosian (2002), we assume that the relativistic spherical shell emits an exponential intrinsic pulse in the form of $j(t) \propto \exp[-t/(5\text{ s})]$ in its comoving frame. To compare with the total occultation case, we take $R_c = 67 R_{\odot}$ and $R_{\text{GRB}} = 10^{15}$ cm, but a lower Lorentz factor $\Gamma = 125$. For a simple demonstration, we further assume that the stellar companion locates at the center within the jet opening angle thus it blocks the central $1/\Gamma$ cone of the jet. The partially occultation light curve is then calculated as

$$I(t) = \int_{\tau_{\text{ang}}/\Gamma_{\text{occ}}^2}^{+\infty} \frac{j(t-x) dx}{(1+x\Gamma^2/\tau_{\text{ang}})^2}, \quad (1)$$

where $\tau_{\text{ang}} \equiv R_{\text{GRB}}/(2c)$ and c is the speed of light. The original light curve in the observer frame can also be calculated through Equation 1 by setting $\Gamma_{\text{occ}} \rightarrow \infty$.

The results are presented in Figure 2. One can see that the observed partially occulted light curve generally mimics the original one, but with a $\sim 25\%$ decrease in the flux. At late times, the observed flux is dominated by the high-latitude emission. Thus, the observed late-time light curve almost coincides with the original one.

The event rate of an occultation (both partial and total) can be estimated as

$$\mathcal{R}_{\text{occ}} \sim \mathcal{R}_{\text{obs}} f_{\text{bin}} f_{d \geq R_{\text{GRB}}} (1/\Gamma + 1/\Gamma_{\text{occ}})^2 / 4, \quad (2)$$

where \mathcal{R}_{obs} is the event rate of GRBs and $f_{d \geq R_{\text{GRB}}}$ is the possibility that $d \geq R_{\text{GRB}}$. Recalling that most Galactic WR binaries have a relatively long orbital period, we conservatively estimate $f_{d \geq R_{\text{GRB}}}$ as 0.2. Taking $\Gamma = 125$ and $\Gamma_{\text{occ}} = 250$, we finally estimate the possibility of a GRB being occulted as $\mathcal{R}_{\text{occ}}/\mathcal{R}_{\text{obs}} \sim 1.4 \times 10^{-6}$.

3.2. Case II

In this case, the GRB emission radius is less than the separation between the GRB central engine and the companion. The observer is off-axis with a viewing angle as θ_{obs} , as illustrated in Figure 1 (observer ii). The observer will miss the original GRB emission but see the reflected radiation by the companion. Note that the observer may also be able to see the original GRB as well as its reflection when the line of sight is near the edge of the GRB jet, especially for a structured jet.

For a GRB with an isotropic energy E_{iso} , the stellar companion receives a total energy input of

$$E_{\text{i,tot}} \simeq E_{\text{iso}} \theta_c^2 / 4, \quad (3)$$

where $\theta_c \equiv R_c/d$ is the angular radius of the companion measured from the GRB central engine. The observer can only see a fraction $(\theta_{\text{obs}}/\pi)$ of the irradiated hemisphere.

Considering the projection effect, the effective energy input integrated over the whole observable reflected energy from irradiated spherical lune can be derived as

$$E_{\text{i}} \simeq \alpha E_{\text{iso}} \theta_c^2 (1 - \cos \theta_{\text{obs}}) / 8. \quad (4)$$

where α is a Bond albedo which defines the reflection efficiency.

Since the incident photons are in gamma-ray energy and the companion surface is relatively cold, the reflection is mainly through the Compton scattering process of the electrons (White et al. 1988; Dermer et al. 1991). The spectrum of the scattered gamma-rays spectrum can be calculated by employing the Green's function $G(\nu', \nu)$ derived by White et al. (1988), which is applicable in our case since $h\nu \ll 66 \text{ MeV}$ hence pair production is negligible. The reflected spectrum is

$$F_{\nu}^{\text{r}}(\nu) = \int G(\nu', \nu) F_{\nu}^{\text{i}}(\nu') d\nu', \quad (5)$$

where $F_{\nu}^{\text{i}}(\nu')$ denotes the incident spectrum, which, in our case, is a Band function (BF; Band et al. 1993) or a cutoff power law (CPL; Campana et al. 2006), with

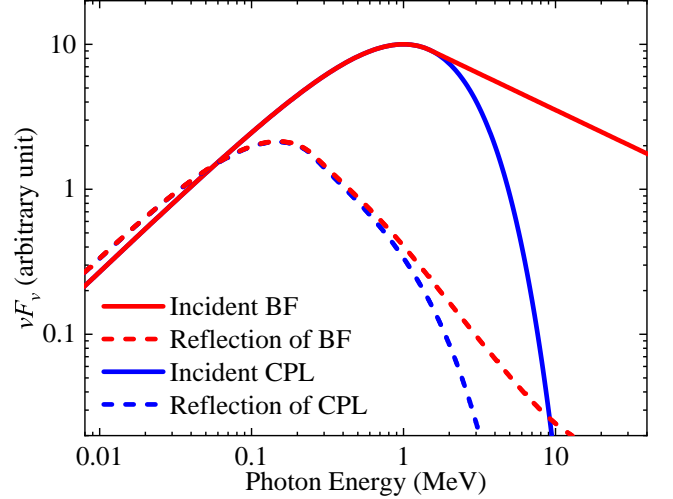


Figure 3. Energy spectra of the incident (solid curves) and reflected (dashed curves) emission. The incident spectrum is assumed to be a Band function (BF, red curves) or a cut-off power-law function (CPL, blue curves). The spectra are normalized to have a peak flux of $\nu F_{\nu} = 10$ for the incident photons, where F_{ν} is the specific flux density at frequency ν .

E_{peak} , the lower and higher energy indices set to 1 MeV, -1 , and -2.5 (for BF only) respectively.

The results are shown in Figure 3. Our calculation shows that the energy flux of the reflected spectrum decreases significantly at higher energies ($> E_{\text{peak}}$) and increases slightly at lower energies. Moreover, the peak photon energy drops by almost one order of magnitude to 143 keV. We also note that the spectrum shape of the reflected emission becomes significantly steeper at the high-energy regime.

The reflection efficiency, α , can be estimated as the fraction of the total fluence of reflection and incident flux integrated over the observed energy range. For a typical BF as show in Figure 3, α is ~ 0.33 for 8 keV–1 MeV for *Fermi*-GBM band (Meegan et al. 2009), and is ~ 0.90 for 15–150 keV *Swift*-BAT band (Barthelmy et al. 2005).

Assuming that the reflected emission is isotropic, the fluence observed by a distant observer can be calculated by Equation 4 as

$$S_{8 \text{ keV} - 1 \text{ MeV}} \sim 10^{-8} \frac{\alpha}{0.2} \frac{E_{\text{iso}}}{10^{54} \text{ erg}} \left(\frac{R_c}{67 R_{\odot}} \frac{10^{15} \text{ cm}}{d} \frac{1 \text{ Gpc}}{D_L} \right)^2 \frac{1+z}{k} (1 - \cos \theta_{\text{obs}}) \text{ erg cm}^{-2}, \quad (6)$$

where D_L is the luminosity distance of the GRB (with $D_L = 1 \text{ Gpc}$ corresponding to a redshift of $z = 0.2$), and k is the k -correction factor. Giving the fact that sensitivity threshold of *Fermi*-GBM detector is about

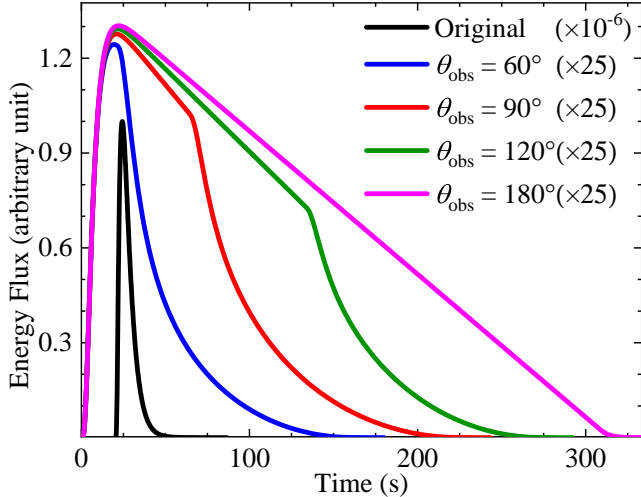


Figure 4. Light curves of the reflected emission produced by a $R_c = 67 R_\odot$ companion viewed at four different angles, i.e., 60° , 90° , 120° , and 180° (blue, red, green, and magenta curves, respectively). The y -axis is normalized so that the original GRB has a peak flux of 10^6 . In this figure, for better illustration, the original GRB (black curve) has been plot after multiplying a factor of 10^{-6} , and it is also right-shifted for 20s.

$\sim 10^{-8} \text{erg cm}^{-2}$ (Kocevski et al. 2018) in the same energy range, we conclude such reflected GRB emission is observable under appropriated parameters, especially for observers at low redshift (e.g., $z \lesssim 0.2$). Since the spectrum (Figure 3) and light curve (see discussion below) shapes of the reflected emission is very similar to the original incident GRB, a distant observer may define the reflected emission as a faint GRB with isotropic energy of

$$E_{\text{iso}}^r \sim 10^{48} \frac{\alpha}{0.2} \frac{E_{\text{iso}}}{10^{54} \text{erg}} \left(\frac{R_c}{67 R_\odot} \frac{10^{15} \text{cm}}{d} \right)^2 (1 - \cos \theta_{\text{obs}}) \text{erg}. \quad (7)$$

The light curve of the reflected emission can be further calculated by considering the high latitude effect of the stellar companion. It takes different times for photons to hit different places of the companion surface and to be reflected toward the observer. As a result, the “reflected” GRB will be broadened to a time scale of $R_c/c \sim 2.3 \text{s} \times R_c/R_\odot$. By considering the projection effect, the exact reflection light curve depends on the viewing angle and can be calculated by

$$I^r(t) = \frac{2}{\pi} \int_0^{\frac{\pi}{2}} \int_{\frac{\pi}{2}-\theta_{\text{obs}}}^{\frac{\pi}{2}} I^i [t - t'(R_c, \theta_{\text{obs}}, \theta, \delta)] \sin^2 \theta \cos \delta \, d\theta \, d\delta, \quad (8)$$

where $t'(R_c, \theta_{\text{obs}}, \theta, \delta)$ is the extra travel time of photons hitting (θ, δ) point on the companion surface, and $I^i(t)$ is the incident light curve. In Figure 4, we plot the

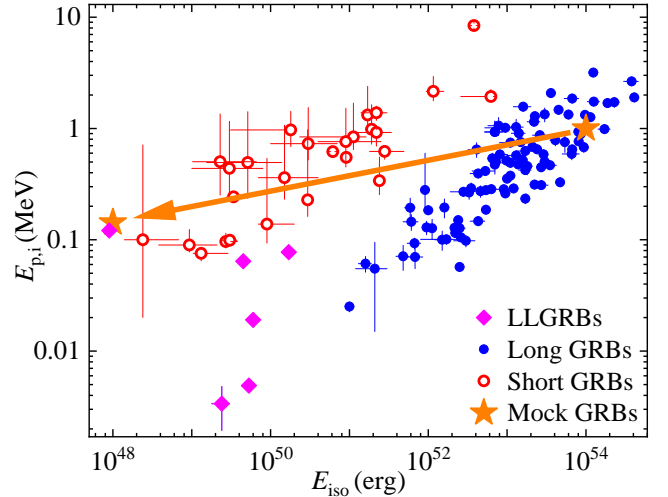


Figure 5. $E_{p,i}$ vs. E_{iso} for low-luminosity GRBs (LLGRBs, diamonds; Zhang 2018), long GRBs (filled circles; Zhang et al. 2018a), and short GRBs (open circles; Zhang et al. 2018a). A mock GRB and its reflection GRB are shown in star symbols, with an arrow pointing from the original mock GRB to the reflected one. All error bars represent $1-\sigma$ uncertainties.

light curves of an original GRB and its reflection emissions viewed at different angles. The companion radius is taken as $67 R_\odot$. We can see that the reflection light curves are broader for larger viewing angles, yet the peak flux is essentially a constant. Moreover, the light curves first decline linearly and break to a convex shape for intermediate viewing angles (e.g., 90° and 120°). This break is due to the equal-time surface effect. When the equal-time surface reaches the edge of the observable irradiated spherical lune, a break occurs. For a small θ_{obs} (e.g., 60°), the linear decline phase is too short (~ 21 s) to be observed in the light curve. On the other hand, for a large viewing angle such as $\theta_{\text{obs}} = 180^\circ$, the break happens at very late stages, and it is not visible on the plot.

Our results shed some light on the origin of low-luminosity GRBs (LLGRBs). LLGRBs are usually considered to form a distinct population of long GRBs (e.g., Liang et al. 2007; Virgili et al. 2009). They have a very low luminosity and relatively soft spectrum (Nakar 2015). The physical origin of LLGRBs is still unresolved. Unlike previous attempts, which involve a special change of the GRB jet radiation or dynamics (e.g., models involving a choked jet, Nakar & Sari 2012; Bromberg et al. 2012; Nakar 2015; a long-lived central engine powering a mildly relativistic jet, Irwin & Chevalier 2016; or the collision between the relativistic ejecta and circumstellar medium, Suzuki et al. 2019), our model, by only introducing the stellar companion’s reflection ef-

fect, can naturally reproduce the observed LLGRBs. This is manifested in Figure 5, where we over-plotted a mock GRB with $E_{\text{iso}} = 10^{54}$ erg and rest-frame peak energy $E_{\text{p,i}} = 1$ MeV and its reflected burst together with a large sample of short and long GRBs, as well as the previously identified LLGRBs (Zhang 2018), on the Amati relation plot (Amati et al. 2002). Interestingly, the reflected GRB shows up as a weak GRB with $E_{\text{p,i}} \sim 143$ keV and $E_{\text{iso}} \sim 10^{48}$ erg and appears in the LLGRB region, closed to GRB 980425 (Kaneko et al. 2007; Liang et al. 2007; Virgili et al. 2009). In addition, we also note that the “reflected” GRBs usually have a long duration (see Figure 4), which is also well consistent with the observed LLGRBs.

Our model predicts a moderate event rate for low-luminosity GRBs. The observed event rate can be estimated as

$$\mathcal{R}_{\text{T}} = \mathcal{R}_{\text{obs}} f_{\text{bin}} f_{d \geq R_{\text{GRB}}}. \quad (9)$$

Typically, we estimate that the observed ratio of low-luminosity GRBs over normal long GRBs is $\mathcal{R}_{\text{T}}/\mathcal{R}_{\text{obs}} \sim 0.04$, which can explain at least a fraction of the observed LLGRBs (e.g., Liang et al. 2007; Virgili et al. 2009).

3.3. Case III

In this case, the GRB emission radius is less than the separation between the GRB central engine and the companion, and the observer is on-axis. However, the companion star is located within the opening angle of the counter jet, as demonstrated as observer iii in Figure 1. It is also equivalent to assign a viewing angle of $\theta_{\text{obs}} = \pi$. The observer will see both the original and the reflected GRBs.

As pointed out by Dermer et al. (1991), the distance between the companion and the GRB central engine will cause a time delay between the original GRB and its reflection. Since the GRB jet moves at a highly relativistic speed, the time delay can be calculated as

$$\tau = \frac{d}{c} (1 - \cos \theta_{\text{obs}}) \sim 6.7 \times 10^4 \frac{d}{10^{15} \text{ cm}} \text{ s}. \quad (10)$$

The reflected emission may manifest as a soft gamma-ray or hard X-ray bump superposed on the GRB high-energy afterglow. Combining with multi-messenger signals such as gravitational waves, the original and reflected GRBs, one may use Equation 10 to further constrain the radiation mechanism through constraining of the prompt emission site by the time delay of the different signals (e.g., Granot et al. 2017; Ioka & Nakamura 2018; Zhang et al. 2018b) if the GRB occurs with a stellar companion.

The observed event rate of such a reflection bump can be estimated as

$$\mathcal{R}_{\text{bump}} = \mathcal{R}_{\text{obs}} f_{\text{bin}} f_{d \geq R_{\text{GRB}}} \theta_{\text{j}}^2 / 4. \quad (11)$$

Taking the jet opening angle as a typical value of 10 degrees, we get $\mathcal{R}_{\text{bump}}/\mathcal{R}_{\text{obs}} \sim 3 \times 10^{-4}$.

3.4. Case IV

In this case, the GRB emission radius is larger than the separation between the GRB central engine and the companion, and the observer is on-axis. Similar to Case (I), the observer will see a dimmer GRB if the companion star does not fully occult the GRB but blocks a $\theta_{\text{c}} = R_{\text{c}}/d$ cone of the jet. The observed light curve is similar to Case (I), but with Γ_{occ} defined as $\Gamma_{\text{occ}} = d/R_{\text{c}}$.

3.5. Case V

In this case, the GRB emission radius is larger than the separation between the GRB central engine and the companion, and the observer is off-axis with a viewing angle of θ_{obs} . The observer will miss the original GRB but will see collision emission between the jet and the companion, probably causing a shock (MacFadyen et al. 2005). The physics behind this scenario is that the relativistic jet materials will collide with the companion, producing a very strong blastwave. The collision will convert the jet kinetic energy into internal energy and generate X-ray emission (MacFadyen et al. 2005). Such emission will not manifest as a GRB but may show up like an X-ray transient.

3.6. Case VI

In this case, the GRB emission radius is larger than the separation between the GRB central engine and the companion, and the observer is on-axis. However, the companion star is located within the opening angle of the counter jet. The geometry configuration is similar to Case (III), and the radiation mechanism is identical to Case (V). Consequently, the observer will see the original GRB, followed by a delayed X-ray transient produced by the relativistic counter jet interacting with the companion star. The X-ray transient may show up as an X-ray flare (e.g., Burrows et al. 2005; Wang et al. 2006; Chincarini et al. 2010; Geng et al. 2017, 2018a), appearing at a time of several hundreds of seconds after the burst (Yi et al. 2016) on top of the X-ray afterglows. Although this collision scenario can hardly produce multiple X-ray flares in a GRB, it may apply to at least a fraction of GRBs with only one single X-ray flare detected.

Besides generating X-ray emission, the collision can also heat the companion star’s atmosphere and expand

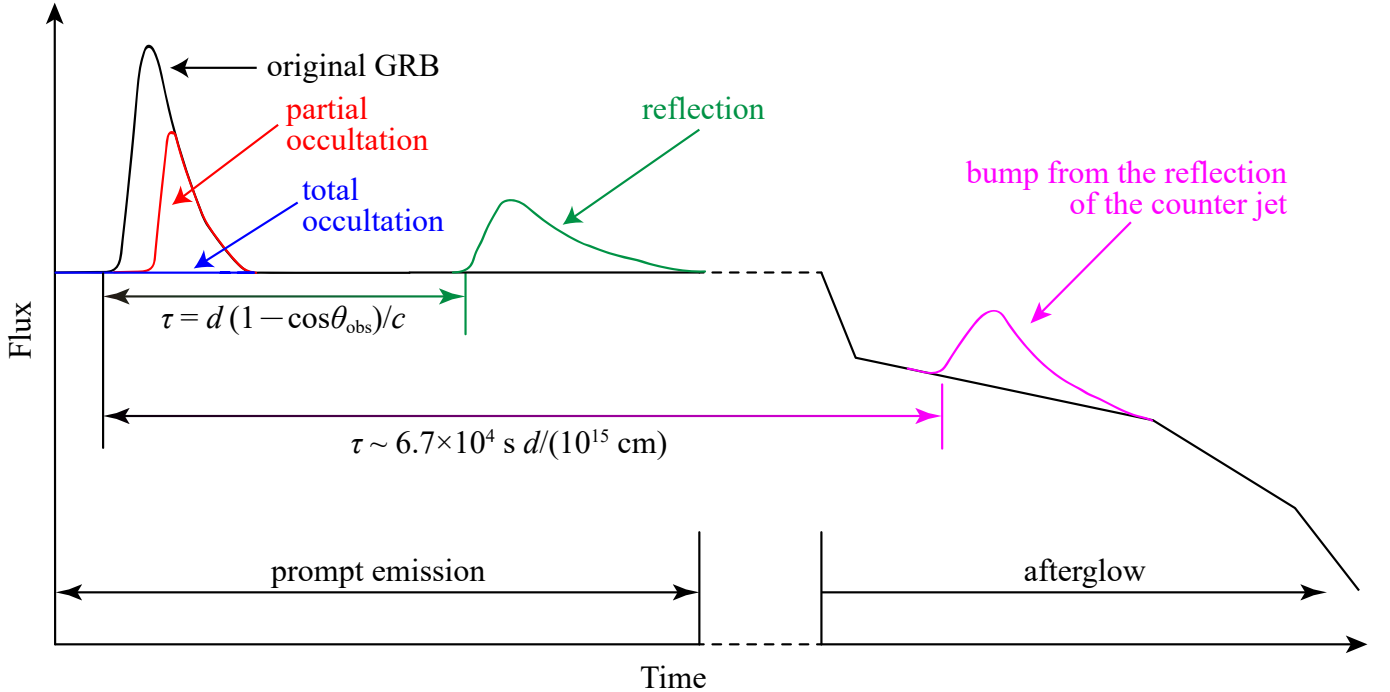


Figure 6. An overall illustration of the various phenomena possibly associated with a GRB that happens in a binary system. The original light curves (solid black curves) of the prompt emission and X-ray afterglow of the GRB are schematically connected by a dashed line. Light curves of the total occultation, partial occultation, reflection, and bumps from the reflection of the counter jet are shown by blue, red, green, and magenta solid curves.

its outer layer. Consequently, an optical/infrared transient may occur after the GRB (MacFadyen et al. 2005). The typical energy of such transient can reach as high as $\sim 10^{48}$ erg (MacFadyen et al. 2005) and may be registered as an early optical flare (Swenson et al. 2013). On the other hand, such a transient is unlikely to be mistaken for a supernova bump because a supernova bump usually shows up about two weeks after the GRB (e.g., Galama et al. 1998; Hjorth et al. 2003), which is much longer than the typical time delay in our scenario (i.e., around one day by Equation 10).

4. SUMMARY AND DISCUSSION

In this paper, we performed a comprehensive study on the effect caused by the stellar companion when a GRB happens in a binary system. Our results are sketched in Figure 6, which illustrates the two main effects, namely occultation and delayed reflection. In addition, we also pointed out that the collision between the jet materials and the stellar companion will generate X-ray emission if the stellar companion is located inside the GRB beam, which is observable by off-axis or counter-on-axis observers.

We note that some additional configurations of the binary system were not included in our analysis. For example, when the companion is partially or entirely outside the jet opening angle (Lu et al. 2015), the

observer can see its inverse-Compton scattered emission, with(without) the original GRB if the observer is on(off)-axis.

GRBs are generally believed to be highly beamed (Rhoads 1997; Huang et al. 1999, 2000a,b,c; Frail et al. 2001; Fong et al. 2015; Wang et al. 2018). Therefore, reflection is expected to be more likely than occultation since an occultation requires the observer to be on-axis. The observational features discussed in this paper can be tested by observations and used to probe the properties of the GRB systems.

We thank the anonymous referee for valuable suggestions that lead to an overall improvement of this study. Z.-C. Z. gratefully acknowledges Yong Shao for helpful discussions on WR stars and Xiangyu Wang for assistance with GRB data. BBZ thanks B. Zhang for helpful discussions on the overall science of this study. This work is supported by National SKA Program of China No. 2020SKA0120300, by the National Natural Science Foundation of China (Grant Nos. 11873030, 12041306, U1938201, U1831135, 11833003, U2038105). B.B.Z acknowledges support by Fundamental Research Funds for the Central Universities (14380046), the science research grants from the China Manned Space Project with NO.CMS-CSST-2021-B11, and the Program for Innovative Talents, Entrepreneur in Jiangsu. We acknowledge the use of public data from the Fermi Science Support Center (FSSC).

Software: Astropy (Astropy Collaboration et al. 2013, 2018), NumPy (van der Walt et al. 2011; Harris et al. 2020), OriginPro (<https://www.originlab.com/>), SciPy (Virtanen et al. 2020)

REFERENCES

- Abbott, B. P., Abbott, R., Abbott, T. D., et al. 2017a, *PhRvL*, 119, 161101, doi: [10.1103/PhysRevLett.119.161101](https://doi.org/10.1103/PhysRevLett.119.161101)
- . 2017b, *ApJL*, 848, L13, doi: [10.3847/2041-8213/aa920c](https://doi.org/10.3847/2041-8213/aa920c)
- Amati, L., Frontera, F., Tavani, M., et al. 2002, *A&A*, 390, 81, doi: [10.1051/0004-6361:20020722](https://doi.org/10.1051/0004-6361:20020722)
- Astropy Collaboration, Robitaille, T. P., Tollerud, E. J., et al. 2013, *A&A*, 558, A33, doi: [10.1051/0004-6361/201322068](https://doi.org/10.1051/0004-6361/201322068)
- Astropy Collaboration, Price-Whelan, A. M., Sipőcz, B. M., et al. 2018, *AJ*, 156, 123, doi: [10.3847/1538-3881/aabc4f](https://doi.org/10.3847/1538-3881/aabc4f)
- Badenes, C., Mazzola, C., Thompson, T. A., et al. 2018, *ApJ*, 854, 147, doi: [10.3847/1538-4357/aaa765](https://doi.org/10.3847/1538-4357/aaa765)
- Band, D., Matteson, J., Ford, L., et al. 1993, *ApJ*, 413, 281, doi: [10.1086/172995](https://doi.org/10.1086/172995)
- Barthelmy, S. D., Barbier, L. M., Cummings, J. R., et al. 2005, *SSRv*, 120, 143, doi: [10.1007/s11214-005-5096-3](https://doi.org/10.1007/s11214-005-5096-3)
- Bromberg, O., Nakar, E., Piran, T., & Sari, R. 2012, *ApJ*, 749, 110, doi: [10.1088/0004-637X/749/2/110](https://doi.org/10.1088/0004-637X/749/2/110)
- Burrows, D. N., Romano, P., Falcone, A., et al. 2005, *Science*, 309, 1833, doi: [10.1126/science.1116168](https://doi.org/10.1126/science.1116168)
- Callingham, J. R., Tuthill, P. G., Pope, B. J. S., et al. 2019, *Nature Astronomy*, 3, 82, doi: [10.1038/s41550-018-0617-7](https://doi.org/10.1038/s41550-018-0617-7)
- Campana, S., Mangano, V., Blustin, A. J., et al. 2006, *Nature*, 442, 1008, doi: [10.1038/nature04892](https://doi.org/10.1038/nature04892)
- Cantiello, M., Yoon, S. C., Langer, N., & Livio, M. 2007, *A&A*, 465, L29, doi: [10.1051/0004-6361:20077115](https://doi.org/10.1051/0004-6361:20077115)
- Chincarini, G., Mao, J., Margutti, R., et al. 2010, *MNRAS*, 406, 2113, doi: [10.1111/j.1365-2966.2010.17037.x](https://doi.org/10.1111/j.1365-2966.2010.17037.x)
- Costa, E., Frontera, F., Heise, J., et al. 1997, *Nature*, 387, 783, doi: [10.1038/42885](https://doi.org/10.1038/42885)
- de Mink, S. E., Cantiello, M., Langer, N., et al. 2009, *A&A*, 497, 243, doi: [10.1051/0004-6361/200811439](https://doi.org/10.1051/0004-6361/200811439)
- Dermer, C. D. 2004, *ApJ*, 614, 284, doi: [10.1086/426532](https://doi.org/10.1086/426532)
- Dermer, C. D., Hurley, K. C., & Hartmann, D. H. 1991, *ApJ*, 370, 341, doi: [10.1086/169820](https://doi.org/10.1086/169820)
- Dsilva, K., Shenar, T., Sana, H., & Marchant, P. 2020, *A&A*, 641, A26, doi: [10.1051/0004-6361/202038446](https://doi.org/10.1051/0004-6361/202038446)
- Duchêne, G., & Kraus, A. 2013, *ARA&A*, 51, 269, doi: [10.1146/annurev-astro-081710-102602](https://doi.org/10.1146/annurev-astro-081710-102602)
- Eichler, D., Livio, M., Piran, T., & Schramm, D. N. 1989, *Nature*, 340, 126, doi: [10.1038/340126a0](https://doi.org/10.1038/340126a0)
- Favata, M., Hughes, S. A., & Holz, D. E. 2004, *ApJL*, 607, L5, doi: [10.1086/421552](https://doi.org/10.1086/421552)
- Fitchett, M. J. 1983, *MNRAS*, 203, 1049, doi: [10.1093/mnras/203.4.1049](https://doi.org/10.1093/mnras/203.4.1049)
- Fong, W., Berger, E., Margutti, R., & Zauderer, B. A. 2015, *ApJ*, 815, 102, doi: [10.1088/0004-637X/815/2/102](https://doi.org/10.1088/0004-637X/815/2/102)
- Fragione, G., Martinez, M. A. S., Kremer, K., et al. 2020, *ApJ*, 900, 16, doi: [10.3847/1538-4357/aba89b](https://doi.org/10.3847/1538-4357/aba89b)
- Frail, D. A., Kulkarni, S. R., Nicastro, L., Feroci, M., & Taylor, G. B. 1997, *Nature*, 389, 261, doi: [10.1038/38451](https://doi.org/10.1038/38451)
- Frail, D. A., Kulkarni, S. R., Sari, R., et al. 2001, *ApJL*, 562, L55, doi: [10.1086/338119](https://doi.org/10.1086/338119)
- Fryer, C. L., & Heger, A. 2005, *ApJ*, 623, 302, doi: [10.1086/428379](https://doi.org/10.1086/428379)
- Galama, T. J., Vreeswijk, P. M., van Paradijs, J., et al. 1998, *Nature*, 395, 670, doi: [10.1038/27150](https://doi.org/10.1038/27150)

- Geng, J.-J., Huang, Y.-F., & Dai, Z.-G. 2017, *ApJL*, 841, L15, doi: [10.3847/2041-8213/aa725a](https://doi.org/10.3847/2041-8213/aa725a)
- Geng, J.-J., Huang, Y.-F., Wu, X.-F., Song, L.-M., & Zong, H.-S. 2018a, *ApJ*, 862, 115, doi: [10.3847/1538-4357/aacd05](https://doi.org/10.3847/1538-4357/aacd05)
- Geng, J.-J., Huang, Y.-F., Wu, X.-F., Zhang, B., & Zong, H.-S. 2018b, *ApJS*, 234, 3, doi: [10.3847/1538-4365/aa9e84](https://doi.org/10.3847/1538-4365/aa9e84)
- Geng, J.-J., Li, B., & Huang, Y.-F. 2021, *The Innovation*, in press, <https://arxiv.org/abs/2103.04165>
- González, J. A., Sperhake, U., Brüggmann, B., Hannam, M., & Husa, S. 2007, *PhRvL*, 98, 091101, doi: [10.1103/PhysRevLett.98.091101](https://doi.org/10.1103/PhysRevLett.98.091101)
- Granot, J., Guetta, D., & Gill, R. 2017, *ApJL*, 850, L24, doi: [10.3847/2041-8213/aa991d](https://doi.org/10.3847/2041-8213/aa991d)
- Hainich, R., Rühling, U., Todt, H., et al. 2014, *A&A*, 565, A27, doi: [10.1051/0004-6361/201322696](https://doi.org/10.1051/0004-6361/201322696)
- Harris, C. R., Millman, K. J., van der Walt, S. J., et al. 2020, *Nature*, 585, 357, doi: [10.1038/s41586-020-2649-2](https://doi.org/10.1038/s41586-020-2649-2)
- Heger, A., Woosley, S. E., & Spruit, H. C. 2005, *ApJ*, 626, 350, doi: [10.1086/429868](https://doi.org/10.1086/429868)
- Hjorth, J., Sollerman, J., Møller, P., et al. 2003, *Nature*, 423, 847, doi: [10.1038/nature01750](https://doi.org/10.1038/nature01750)
- Horvat, M., Conroy, K. E., Pablo, H., et al. 2018, *ApJS*, 237, 26, doi: [10.3847/1538-4365/aacd0f](https://doi.org/10.3847/1538-4365/aacd0f)
- Huang, X.-L., Liang, E.-W., Liu, R.-Y., Cheng, J.-G., & Wang, X.-Y. 2020, *ApJL*, 903, L26, doi: [10.3847/2041-8213/abc330](https://doi.org/10.3847/2041-8213/abc330)
- Huang, Y. F., Dai, Z. G., & Lu, T. 1999, *MNRAS*, 309, 513, doi: [10.1046/j.1365-8711.1999.02887.x](https://doi.org/10.1046/j.1365-8711.1999.02887.x)
- . 2000a, *A&A*, 355, L43
- . 2000b, *MNRAS*, 316, 943, doi: [10.1046/j.1365-8711.2000.03683.x](https://doi.org/10.1046/j.1365-8711.2000.03683.x)
- . 2002, *MNRAS*, 332, 735, doi: [10.1046/j.1365-8711.2002.05334.x](https://doi.org/10.1046/j.1365-8711.2002.05334.x)
- Huang, Y. F., Gou, L. J., Dai, Z. G., & Lu, T. 2000c, *ApJ*, 543, 90, doi: [10.1086/317076](https://doi.org/10.1086/317076)
- Ioka, K., & Nakamura, T. 2018, *Progress of Theoretical and Experimental Physics*, 2018, 043E02, doi: [10.1093/ptep/pty036](https://doi.org/10.1093/ptep/pty036)
- Irwin, C. M., & Chevalier, R. A. 2016, *MNRAS*, 460, 1680, doi: [10.1093/mnras/stw1058](https://doi.org/10.1093/mnras/stw1058)
- Izzard, R. G., Ramirez-Ruiz, E., & Tout, C. A. 2004, *MNRAS*, 348, 1215, doi: [10.1111/j.1365-2966.2004.07436.x](https://doi.org/10.1111/j.1365-2966.2004.07436.x)
- Justesen, A. B., & Albrecht, S. 2020, *A&A*, 642, A212, doi: [10.1051/0004-6361/202039138](https://doi.org/10.1051/0004-6361/202039138)
- Kaneko, Y., Ramirez-Ruiz, E., Granot, J., et al. 2007, *ApJ*, 654, 385, doi: [10.1086/508324](https://doi.org/10.1086/508324)
- Kocevski, D., Ryde, F., & Liang, E. 2003, *ApJ*, 596, 389, doi: [10.1086/377707](https://doi.org/10.1086/377707)
- Kocevski, D., Burns, E., Goldstein, A., et al. 2018, *ApJ*, 862, 152, doi: [10.3847/1538-4357/aacb7b](https://doi.org/10.3847/1538-4357/aacb7b)
- Kouveliotou, C., Meegan, C. A., Fishman, G. J., et al. 1993, *ApJL*, 413, L101, doi: [10.1086/186969](https://doi.org/10.1086/186969)
- Kumar, P., & Zhang, B. 2015, *PhR*, 561, 1, doi: [10.1016/j.physrep.2014.09.008](https://doi.org/10.1016/j.physrep.2014.09.008)
- Levan, A., Crowther, P., de Grijs, R., et al. 2016, *SSRv*, 202, 33, doi: [10.1007/s11214-016-0312-x](https://doi.org/10.1007/s11214-016-0312-x)
- Liang, E., Zhang, B., Virgili, F., & Dai, Z. G. 2007, *ApJ*, 662, 1111, doi: [10.1086/517959](https://doi.org/10.1086/517959)
- Liang, E.-W., Yi, S.-X., Zhang, J., et al. 2010, *ApJ*, 725, 2209, doi: [10.1088/0004-637X/725/2/2209](https://doi.org/10.1088/0004-637X/725/2/2209)
- London, R. A., & Cominsky, L. R. 1983, *ApJL*, 275, L59, doi: [10.1086/184171](https://doi.org/10.1086/184171)
- Lu, W., Kumar, P., & Smoot, G. F. 2015, *MNRAS*, 453, 1458, doi: [10.1093/mnras/stv1677](https://doi.org/10.1093/mnras/stv1677)
- MacFadyen, A. I., Ramirez-Ruiz, E., & Zhang, W. 2005, *arXiv e-prints*, astro, <https://arxiv.org/abs/astro-ph/0510192>
- MacFadyen, A. I., & Woosley, S. E. 1999, *ApJ*, 524, 262, doi: [10.1086/307790](https://doi.org/10.1086/307790)
- Mason, B. D., Hartkopf, W. I., Gies, D. R., Henry, T. J., & Helsel, J. W. 2009, *AJ*, 137, 3358, doi: [10.1088/0004-6256/137/2/3358](https://doi.org/10.1088/0004-6256/137/2/3358)
- Meegan, C., Lichti, G., Bhat, P. N., et al. 2009, *ApJ*, 702, 791, doi: [10.1088/0004-637X/702/1/791](https://doi.org/10.1088/0004-637X/702/1/791)
- Merritt, D., Milosavljević, M., Favata, M., Hughes, S. A., & Holz, D. E. 2004, *ApJL*, 607, L9, doi: [10.1086/421551](https://doi.org/10.1086/421551)
- Nakar, E. 2007, *PhR*, 442, 166, doi: [10.1016/j.physrep.2007.02.005](https://doi.org/10.1016/j.physrep.2007.02.005)
- . 2015, *ApJ*, 807, 172, doi: [10.1088/0004-637X/807/2/172](https://doi.org/10.1088/0004-637X/807/2/172)
- Nakar, E., & Sari, R. 2012, *ApJ*, 747, 88, doi: [10.1088/0004-637X/747/2/88](https://doi.org/10.1088/0004-637X/747/2/88)
- Narayan, R., Paczynski, B., & Piran, T. 1992, *ApJL*, 395, L83, doi: [10.1086/186493](https://doi.org/10.1086/186493)
- Paczynski, B. 1967, *AcA*, 17, 355
- Petrovic, J., Langer, N., Yoon, S. C., & Heger, A. 2005, *A&A*, 435, 247, doi: [10.1051/0004-6361:20042545](https://doi.org/10.1051/0004-6361:20042545)
- Planck Collaboration, Aghanim, N., Akrami, Y., et al. 2020, *A&A*, 641, A6, doi: [10.1051/0004-6361/201833910](https://doi.org/10.1051/0004-6361/201833910)
- Rappaport, S. A., & Joss, P. C. 1985, *Nature*, 314, 242, doi: [10.1038/314242a0](https://doi.org/10.1038/314242a0)
- Rhoads, J. E. 1997, *ApJL*, 487, L1, doi: [10.1086/310876](https://doi.org/10.1086/310876)
- Rosslowe, C. K., & Crowther, P. A. 2015, *MNRAS*, 447, 2322, doi: [10.1093/mnras/stu2525](https://doi.org/10.1093/mnras/stu2525)
- Ryde, F., & Petrosian, V. 2002, *ApJ*, 578, 290, doi: [10.1086/342271](https://doi.org/10.1086/342271)

- Shenar, T., Hainich, R., Todt, H., et al. 2016, *A&A*, 591, A22, doi: [10.1051/0004-6361/201527916](https://doi.org/10.1051/0004-6361/201527916)
- Suzuki, A., Maeda, K., & Shigeyama, T. 2019, *ApJ*, 870, 38, doi: [10.3847/1538-4357/aaef85](https://doi.org/10.3847/1538-4357/aaef85)
- Swenson, C. A., Roming, P. W. A., De Pasquale, M., & Oates, S. R. 2013, *ApJ*, 774, 2, doi: [10.1088/0004-637X/774/1/2](https://doi.org/10.1088/0004-637X/774/1/2)
- Uhm, Z. L., & Zhang, B. 2015, *ApJ*, 808, 33, doi: [10.1088/0004-637X/808/1/33](https://doi.org/10.1088/0004-637X/808/1/33)
- van der Hucht, K. A. 2001, *NewAR*, 45, 135, doi: [10.1016/S1387-6473\(00\)00112-3](https://doi.org/10.1016/S1387-6473(00)00112-3)
- van der Walt, S., Colbert, S. C., & Varoquaux, G. 2011, *Computing in Science and Engineering*, 13, 22, doi: [10.1109/MCSE.2011.37](https://doi.org/10.1109/MCSE.2011.37)
- van Meter, J. R., Miller, M. C., Baker, J. G., Boggs, W. D., & Kelly, B. J. 2010, *ApJ*, 719, 1427, doi: [10.1088/0004-637X/719/2/1427](https://doi.org/10.1088/0004-637X/719/2/1427)
- van Paradijs, J., Groot, P. J., Galama, T., et al. 1997, *Nature*, 386, 686, doi: [10.1038/386686a0](https://doi.org/10.1038/386686a0)
- Virgili, F. J., Liang, E.-W., & Zhang, B. 2009, *MNRAS*, 392, 91, doi: [10.1111/j.1365-2966.2008.14063.x](https://doi.org/10.1111/j.1365-2966.2008.14063.x)
- Virtanen, P., Gommers, R., Oliphant, T. E., et al. 2020, *Nature Methods*, 17, 261, doi: [10.1038/s41592-019-0686-2](https://doi.org/10.1038/s41592-019-0686-2)
- Wang, X.-G., Zhang, B., Liang, E.-W., et al. 2018, *ApJ*, 859, 160, doi: [10.3847/1538-4357/aabc13](https://doi.org/10.3847/1538-4357/aabc13)
- Wang, X.-Y., Li, Z., & Mészáros, P. 2006, *ApJL*, 641, L89, doi: [10.1086/504151](https://doi.org/10.1086/504151)
- White, T. R., Lightman, A. P., & Zdziarski, A. A. 1988, *ApJ*, 331, 939, doi: [10.1086/166611](https://doi.org/10.1086/166611)
- Woosley, S. E. 1993, *ApJ*, 405, 273, doi: [10.1086/172359](https://doi.org/10.1086/172359)
- Woosley, S. E., & Heger, A. 2006, *ApJ*, 637, 914, doi: [10.1086/498500](https://doi.org/10.1086/498500)
- Yi, S.-X., Xi, S.-Q., Yu, H., et al. 2016, *ApJS*, 224, 20, doi: [10.3847/0067-0049/224/2/20](https://doi.org/10.3847/0067-0049/224/2/20)
- Yoon, S. C., Dierks, A., & Langer, N. 2012, *A&A*, 542, A113, doi: [10.1051/0004-6361/201117769](https://doi.org/10.1051/0004-6361/201117769)
- Yoon, S. C., & Langer, N. 2005, *A&A*, 443, 643, doi: [10.1051/0004-6361:20054030](https://doi.org/10.1051/0004-6361:20054030)
- Zhang, B. 2018, *The Physics of Gamma-Ray Bursts* (Cambridge University Press), doi: [10.1017/9781139226530](https://doi.org/10.1017/9781139226530)
- Zhang, B., Wang, Y., & Li, L. 2021, *ApJL*, 909, L3, doi: [10.3847/2041-8213/abe6ab](https://doi.org/10.3847/2041-8213/abe6ab)
- Zhang, B., & Yan, H. 2011, *ApJ*, 726, 90, doi: [10.1088/0004-637X/726/2/90](https://doi.org/10.1088/0004-637X/726/2/90)
- Zhang, B. B., Zhang, B., Castro-Tirado, A. J., et al. 2018a, *Nature Astronomy*, 2, 69, doi: [10.1038/s41550-017-0309-8](https://doi.org/10.1038/s41550-017-0309-8)
- Zhang, B. B., Zhang, B., Sun, H., et al. 2018b, *Nature Communications*, 9, 447, doi: [10.1038/s41467-018-02847-3](https://doi.org/10.1038/s41467-018-02847-3)